JHEP

Published for SISSA by Springer

Received: March 4, 2016
Revised: May 4, 2016
Accepted: May 15, 2016
Published: May 20, 2016

# Enhancing the Higgs associated production with a top quark pair

**Marcin Badziak**[a] **and Carlos E.M. Wagner**[b,c,d]

[a] *Institute of Theoretical Physics, Faculty of Physics, University of Warsaw, ul. Pasteura 5, PL-02-093 Warsaw, Poland*

[b] *Enrico Fermi Institute, University of Chicago, Chicago, IL 60637, U.S.A.*

[c] *High Energy Physics Division, Argonne National Laboratory, Argonne, IL 60439, U.S.A.*

[d] *Kavli Institute for Cosmological Physics, University of Chicago, Chicago, IL 60637, U.S.A.*

*E-mail:* mbadziak@fuw.edu.pl, cwagner@hep.anl.gov

Abstract: It is pointed out that in a wide class of models reminiscent of type-II Two-Higgs-Doublet Models (2HDM) the signal of the Higgs produced in association with a top-antitop quark pair ($tth$) and decaying into gauge bosons can be significantly larger than the Standard Model (SM) prediction without violating any experimental constraints. The crucial feature of these models is enhanced (suppressed) Higgs coupling to top (bottom) quarks and existence of light colored particles that give negative contribution to the effective Higgs coupling to gluons resulting in the gluon fusion rates in the gauge boson decay channels close to SM predictions. We demonstrate this mechanism in NMSSM with light stops and show that $tth$ signal in the $WW$ decay channel can be two times larger than the SM prediction, as suggested by the excesses observed by ATLAS and CMS, provided that the Higgs-singlet superpotential coupling $\lambda \gtrsim 0.8$ and the MSSM-like Higgs boson masses are in the range of 160 to 300 GeV.

Keywords: Beyond Standard Model, Higgs Physics, Supersymmetric Standard Model

ArXiv ePrint: 1602.06198



doi:10.1007/JHEP05(2016)123

JHEP05(2016)123

## Contents


**1 Introduction** 1

**2 tth in type-II 2HDM** 3

**3 tth in type-II 2HDM with light stops** 5

**4 tth in the NMSSM** 7

**5 Conclusions** 15

**A Higgs signal rate computation** 16


## 1 Introduction

The most important legacy of the first run of the LHC is the discovery of a 125 GeV Higgs boson [1, 2]. The measured Higgs signal rates in all channels agree with the SM prediction at $2\sigma$ level [3]. Moreover, in the most precisely measured channels, such as gluon fusion ones with a Higgs decaying into gauge bosons, the agreement is typically at the $1\sigma$ level. One of the main goals of the 13 TeV LHC is to improve measurements of the Higgs properties. However, the possibility of extracting information on new physics from measurements of Higgs rates in the gluon fusion production channels is somewhat limited by systematics and the theoretical uncertainty of the SM gluon fusion production cross-section [4–8]. One can then naturally ask whether there are better channels for the discovery of New Physics from Higgs measurements at the LHC. Fortunately, the rate measurements in some channels are currently statistically limited and can benefit a lot from the high luminosity expected to be delivered by the 13 TeV LHC. Among these channels, a particularly interesting one is the Higgs production in association with a top-antitop quark pair ($tth$).

The top quark is often considered as a window to New Physics. This statement is supported by the fact that the top quark mass is much larger than all other quarks and its SM Yukawa coupling is of order unity. In consequence, there are many phenomena involving quarks that are measured (or can be measured in a near future) only for top quarks. That said, it should be emphasized that the top quark Yukawa coupling has not been measured directly so far. The only hint that the top quark Yukawa coupling is indeed very close to the SM prediction comes from the measurements of the Higgs gluon fusion production rates that agree very well with the SM. In the SM, the gluon fusion production cross-section is to a large extent controlled by the top quark Yukawa coupling. However, in many extensions of the SM there are new coloured particles that can contribute to the gluon fusion cross-section, interfering with the top quark loop. In such a case, simple relation



JHEP05(2016)123

between the top quark Yukawa coupling and the gluon fusion production cross-section is lost.[1] Therefore, in general it is the $tth$ production which may give access to the top quark Yukawa coupling directly.

A particularly interesting and timely question at the dawn of the 13 TeV LHC run is whether the $tth$ signal rates can be substantially enhanced with respect to the SM prediction. If a big enhancement is indeed realized in Nature we should discover it at the LHC run two. Moreover, the LHC data from the first run give some hints for such enhancement since a fit to the combined ATLAS and CMS data yields a signal strength

$$\mu^{\rm tth} = 2.3^{+0.7}_{-0.6}, \tag{1.1}$$

for the $tth$ production cross-section normalised to the SM prediction [3]. Many different final states contribute to this enhancement, both at ATLAS [11, 12] and CMS [13], but the most significant excesses are observed in multilepton final states which probe mainly the $tth$ production in the $WW$ decay channel. For the $\gamma\gamma$ channel the central values are also above the SM prediction in both experiments, with particularly large enhancement observed at CMS. All of the above suggests enhancement of $tth$ signal rates with a Higgs decaying into gauge bosons.

During the last year, there have been several analyses that interpreted the excess in the $tth$ searches in New Physics models. Most of those works focused on the same-sign dilepton excess in the $tth$ searches and interpreted it as a signature of a new particle, see e.g. refs. [14, 15]. To the best of our knowlegde, only ref. [16] interpreted the $tth$ excess in a model with enhanced Higgs coupling to top quarks.

In the present paper we show that the $tth$ production rate with a Higgs decaying into gauge boson can be more than a factor of two larger than in the SM without violating any existing data in a wide class of models reminiscent of type-II Two-Higgs-Doublet Models (2HDM). In order to achieve this, the existence of new light coloured particles is necessary to disentangle the top quark Yukawa coupling from the effective Higgs coupling to gluons. We demonstrate this effect using stops as an example which, if sufficiently light and highly mixed, can reduce the effective Higgs coupling to gluons keeping gluon fusion rates close to the SM prediction when the $tth$ production channel is enhanced. We also show that such a big $tth$ enhancement can be accommodated in the Next-to-Minimal Supersymmetric Standard Model (NMSSM) [17] if the Higgs-singlet superpotential coupling $\lambda$ is large enough and the MSSM-like Higgs bosons are in the range of several hundreds of GeV.

The rest of the paper is organized as follows. In section 2 we study the $tth$ signal rates in type-II 2HDM and show that its possible enhancement is very limited by the Higgs data in the gluon fusion production channels. In section 3 we add light stops to type-II 2HDM and show that large $tth$ enhancement can be consistent with the experimental data. In section 4 we show that such enhancement is possible in NMSSM and discuss implications for the spectrum of MSSM-like Higgses taking into account experimental constraints and present several benchmark points. We summarize our results in section 5.

[1] The degeneracy in the gluon fusion production cross-section between the top quark and New Physics contributions can be broken by studying production of a boosted Higgs with a jet [9, 10].



JHEP05(2016)123

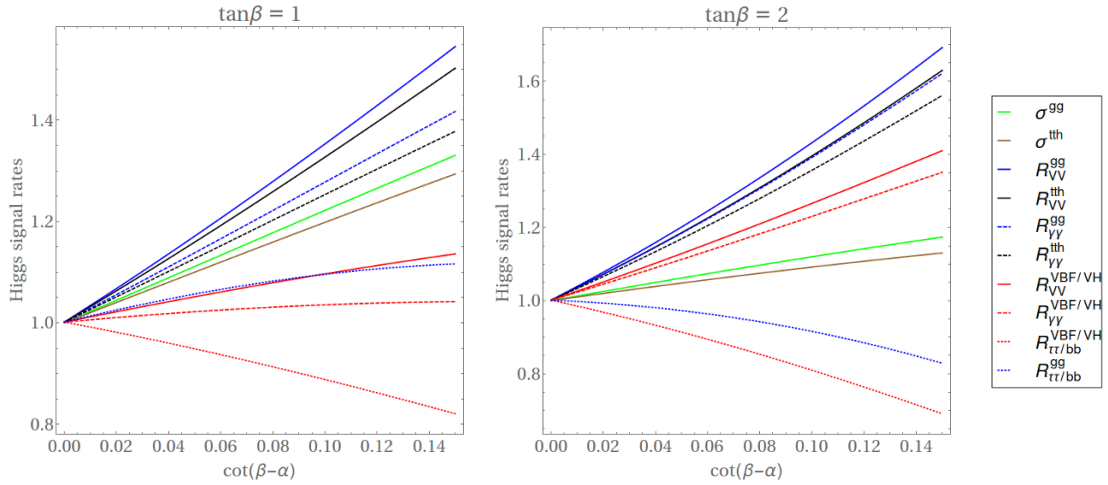


**Figure 1**. Dependence of Higgs signal rates on $\cot(\beta-\alpha)$ for $\tan\beta = 1$ (left) and 2 (right) in type-II 2HDM.

## 2 tth in type-II 2HDM

Let us start with an analysis of type-II 2HDM which mimics certain regions of the MSSM, as well as the NMSSM with decoupled singlet. The tth production cross-section is controlled by the top quark Yukawa coupling. Since the SM Higgs production cross-sections are computed with better precision than in any of the SM extensions we focus on the tth production cross-section normalised to the SM prediction:

$$\sigma^{tth} \equiv \frac{\sigma(gg \to tth)}{\sigma^{\rm SM}(gg \to tth)} = c_t^2 \,, \tag{2.1}$$

where $c_t$ is the top quark Yukawa coupling normalised to its SM value.

The LHC experiments measure the production cross-section times branching ratio so it is useful to define theoretically predicted signal strengths modifiers as:

$$R_i^j \equiv \frac{\sigma^j \times {\rm BR}(h \to i)}{\sigma^{j\rm SM} \times {\rm BR}^{\rm SM}(h \to i)} \,. \tag{2.2}$$

Throughout the paper, we distinguish the theoretical predictions for the signal strengths from the corresponding LHC measurements, that we define in the conventional way as $\mu_i^j$. In the present case $R_i^j$ depend on the Higgs couplings to up-type fermions $c_t$, down-type fermions $c_b$ and massive gauge bosons $c_V$, as well as on effective Higgs couplings to gluons and photons that depend on the SM couplings and may receive contributions from New Physics. Formulae for $R_i^j$ as a function of these couplings are given in the appendix.

In the type-II 2HDM the couplings (normalised to SM) read:

$$c_t = \frac{\cos\alpha}{\sin\beta} = \sin(\beta-\alpha) + \cot\beta\cos(\beta-\alpha) \,, \tag{2.3}$$

$$c_b = -\frac{\sin\alpha}{\cos\beta} = \sin(\beta-\alpha) - \tan\beta\cos(\beta-\alpha) \,, \tag{2.4}$$

$$c_V = \sin(\beta-\alpha) \,, \tag{2.5}$$



JHEP05(2016)123

| Channel | ATLAS+CMS combined result |
|---|---|
| $\mu^{\rm gg}_{\gamma\gamma}$ | $1.19^{+0.28}_{-0.25}$ |
| $\mu^{\rm gg}_{ZZ}$ | $1.44^{+0.38}_{-0.34}$ |
| $\mu^{\rm gg}_{WW}$ | $1.00^{+0.23}_{-0.20}$ |
| $\mu^{\rm gg}_{\tau\tau}$ | $1.10^{+0.61}_{-0.58}$ |
| $\mu^{\rm gg}_{bb}$ | $1.09^{+0.93}_{-0.89}$ |
| $\mu^{\rm VBF/VH}_{\gamma\gamma}$ | $1.05^{+0.44}_{-0.41}$ |
| $\mu^{\rm VBF/VH}_{ZZ}$ | $0.48^{+1.37}_{-0.91}$ |
| $\mu^{\rm VBF/VH}_{WW}$ | $1.38^{+0.41}_{-0.37}$ |
| $\mu^{\rm VBF/VH}_{\tau\tau}$ | $1.12^{+0.37}_{-0.35}$ |
| $\mu^{\rm VBF/VH}_{bb}$ | $0.65^{+0.30}_{-0.29}$ |

**Table 1**. Observed Higgs signal strengths from the combination of the ATLAS and CMS data, corresponding to table 13 of ref. [3].

The SM couplings are obtained in the decoupling limit $\alpha = \beta - \pi/2$. It is clear from the above formulae that significant deviations from the SM for the $tth$ production cross-section can only occur for small values of $\tan\beta$ and away from the decoupling limit. This generically implies relatively small mass of additional Higgs bosons, especially in weakly-coupled models of new physics where $\cos(\beta-\alpha) \sim M_Z^2/m_H^2$ is typically expected. It is important to note the anti-correllation between $c_t$ and $c_b$. If one is enhanced, the other one is suppressed and vice-versa. Moreover, for $\tan\beta > 1$ the bottom Yukawa coupling deviates from the SM more than the top quark Yukawa. This is particularly important since the bottom Yukawa coupling controls to large extent the total decay width of the Higgs because the SM Higgs branching ratio to bottom and tau pairs exceeds in total 60%. Therefore, all the branching ratios strongly deviate from the SM prediction if $c_b$ strongly deviates from $c_V$. Since the LHC Higgs measurements are close to the SM predictions this puts strong constraint on possible deviations of $c_t$ from one.

The dependence of $\sigma^{tth}$ and other rates on $\cot(\beta-\alpha)$ for $\tan\beta = 1$ and 2 is shown in figure 1. Due to the observed excess in $\mu^{\rm tth}_{WW}$, it is particularly interesting to investigate predictions for $R^{\rm tth}_{VV}$, where $V = W$ or $Z$. It can be seen from eqs. (2.3)–(2.4) that in type-II 2HDM $R^{\rm tth}_{VV}$ can be enhanced only for $\cot(\beta-\alpha) > 0$. As is shown in figure 1, in such a case, both the $tth$ production cross-section and the branching ratio to $WW$ is enhanced. However, a large enhancement of $R^{\rm tth}_{VV}$ is constrained by the existing LHC Higgs data which in most cases agree quite well with the SM predictions. For easy comparison we reproduce the result of the fit to the combined ATLAS and CMS data in table 1. The main constraint comes from the measurements of $R^{\rm gg}_{VV}$ which is even slightly bigger than $R^{\rm tth}_{VV}$ because the enhancement of the gluon-fusion cross section becomes bigger than the one of the $tth$ cross-section when the $hb\bar{b}$ coupling is suppressed, cf. eqs. (A.6) and (A.9).

We conclude that in type-II 2HDM, without the addition of new particles, it is not possible to strongly enhance $R^{\rm tth}_{VV}$ while keeping other rates in a good agreement with the SM predictions.



JHEP05(2016)123

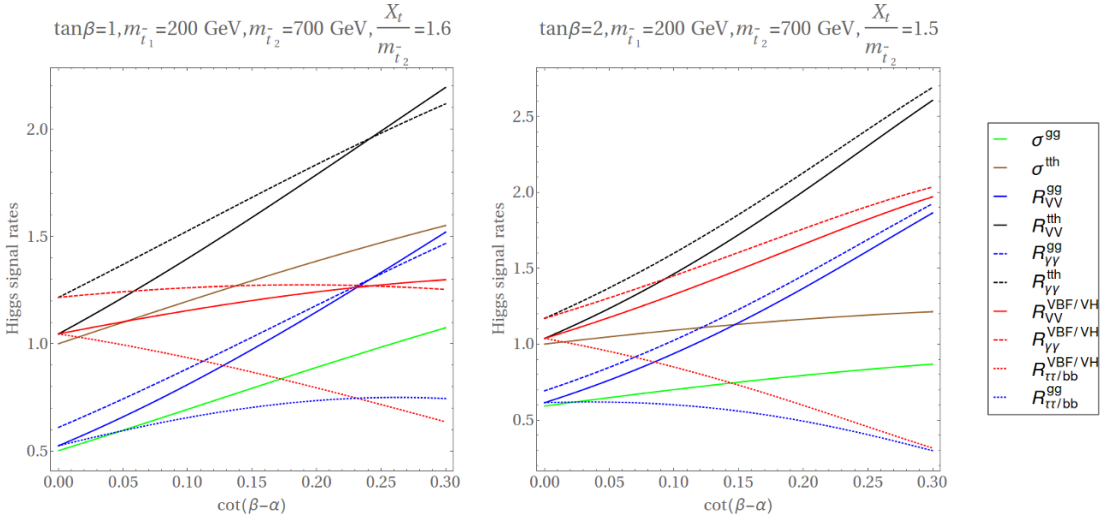


**Figure 2**. Dependence of the Higgs signal rates on $\cot(\beta-\alpha)$ for $\tan\beta = 1$ and 2 in type-II 2HDM with light stops.

## 3 tth in type-II 2HDM with light stops

The conclusion of the previous section would not hold if there existed new coloured states that modify gluon-fusion production cross-section. Such modification of effective coupling of the Higgs to gluons is parameterised by $\delta c_g$ in our computation of the cross sections and branching ratios given in eq. (A.9). In this paper we focus on light stops as a source of $\delta c_g$ because the Higgs sector of minimal SUSY models reduces to the class of Type-II 2HDM in certain limits. Nevertheless, one should keep in mind that modification of $c_g$ can originate from other light coloured states, see e.g. ref. [18], so the mechanism we present is applicable more generally.

Type-II 2HDM with light stops that we consider should be thought of a simplified model of an extended model which reduces to the MSSM at low energies. One example that we shall analyze below is the NMSSM in which the singlet is decoupled and does not effectively mix with the Higgs doublets. Note that an ultraviolet completion to the MSSM is needed because for small $\tan\beta$ light stops cannot account for the 125 GeV Higgs mass.

Light stops modify the effective Higgs coupling to gluons and photons in the following way, see e.g. refs. [18, 19]:

$$\frac{c_g}{c_g^{\rm SM}} = \frac{c_\gamma}{c_\gamma^{\rm SM}} = c_t + \frac{m_t^2}{4}\left[c_t\left(\frac{1}{m^2_{\tilde{t}_1}}+\frac{1}{m^2_{\tilde{t}_2}}\right) - \frac{\tilde{X}_t^2}{m^2_{\tilde{t}_1}\, m^2_{\tilde{t}_2}}\right], \tag{3.1}$$

where $\tilde{X}_t^2 \equiv X_t\left(A_t\frac{\cos\alpha}{\sin\beta}+\mu\frac{\sin\alpha}{\sin\beta}\right)$ with the stop mixing parameter given by $X_t \equiv A_t - \mu/\tan\beta$ (note: in the decoupling limit $\tilde{X}_t^2 = X_t^2$). In the above formula the corrections of order $\mathcal{O}(m_h/m_{\tilde{t}})$ are neglected because they have very small impact on the results already for stop masses of about 200 GeV. We also neglect the NLO QCD corrections which have a rather small effect on the results [19, 20].

In order to enhance the $tth$ production channel keeping the gluon fusion rates close to its SM values the effective Higgs coupling to gluons must be smaller than the Higgs coupling to



JHEP05(2016)123

top quark. It should be clear from eq. (3.1) that for relatively large stop mixing parameters, $\frac{\tilde{X}_t^2}{m^2_{\tilde{t}_2}} \gtrsim c_t$, the modification of the gluon coupling $c_g/c_g^{\rm SM}$ can be smaller than $c_t$. In this cases $R^{\rm gg}_{VV} < R^{\rm tth}_{VV}$, as required by data. In the left panel of figure 2 we show an example with stop masses of 200 and 700 GeV and $\tan\beta = 1$. As can be seen from this figure, values of $R^{\rm tth}_{VV}$ of about 2 are possible while keeping $R^{\rm gg}_{VV}$ and $R^{\rm gg}_{\gamma\gamma}$ only 30% above the SM prediction, which is within the present $1\sigma$ experimental bounds for these Higgs production channels [3], see also point B1 in table 2. Notice also that for $R^{\rm tth}_{VV} \approx 2$ the Higgs $tth$ production cross-section $\sigma^{\rm tth}$ is enhanced by about 45% while the rest of the enhancement originates from suppressed $hb\bar{b}$ coupling that results in enhanced $\mathrm{BR}(h \to VV)$. Another consequence of suppressed $hb\bar{b}$ coupling are suppressed Higgs decays to $b\bar{b}$ and $\tau\tau$. Nevertheless, for $\tan\beta = 1$ the signal strengths in these decay channels are about 0.75 (in gluon fusion production mode, as well as in the Higgs associated production with a weak boson (VH) and weak boson fusion (VBF) production channels). Such small suppression is even preferred by the current LHC measurements of the $b\bar{b}$ decay channel. Similar suppression is not observed in the $\tau\tau$ decay channel but values of $R^{\rm VBF/VH}_{\tau\tau}$ as low as about 0.4 are allowed at $2\sigma$ level for the VBF/VH production channel. The gluon fusion rate in the $\tau\tau$ channel is poorly measured and even zero is allowed at $2\sigma$ level.

As $\tan\beta$ increases, suppression of the $hb\bar{b}$ coupling becomes stronger while the enhancement of the $ht\bar{t}$ coupling becomes weaker. In consequence, enhancement of $R^{\rm tth}_{VV}$ is mainly driven by enhancement of $\mathrm{BR}(h \to VV)$. This is demonstrated for $\tan\beta = 2$ in the right panel of figure 2. In this case $R^{\rm tth}_{VV} = 2$ is obtained with $\sigma^{\rm tth}$ only 20% above the SM prediction. This results in larger deviations of other signal rates from the SM predictions. The gluon fusion production rate in the gauge bosons decay channel is not an issue because it can be adjusted to SM-like values by appropriate choice of $X_t/m_{\tilde{t}_2}$. The gluon fusion rate in the $\tau\tau$ turns out to be quite low but it poses no tension with the current LHC data. Constraints from the VBF/VH production channels are more important since these channels are not affected by presence of light stops. VH is the most relevant production channel for $h \to b\bar{b}$ while for $h \to \tau\tau$ this is VBF. As long as $\tan\beta \lesssim 1.5$, $R^{\rm VBF/VH}_{\tau\tau}$ sets the strongest upper limit on $R^{\rm tth}_{VV}$.

For the Higgs decaying to gauge bosons VH and VBF channels are measured much less precisely than the gluon fusion one. Nevertheless, for $\tan\beta \gtrsim 1.5$ these channels start to compete with $R^{\rm VBF/VH}_{\tau\tau}$ in setting an upper limit on possible enhancement of $R^{\rm tth}_{VV}$, as can be seen from figure 3 and table 2 with benchmark points. Currently the strongest upper limit on signal rates in these production channels is about 1.9 (1.5) at $2\sigma$ ($1\sigma$) for $R^{\rm VBF/VH}_{\gamma\gamma}$. Moreover, if the gluon fusion rate is suppressed by light stops then $\Gamma(h \to \gamma\gamma)$ is enhanced which makes this channel even more important. Nevertheless, for $\tan\beta = 2$ it is still possible to obtain $R^{\rm tth}_{VV} \sim 2$ while keeping other rates within $2\sigma$ from the experimental central values. For large enough $\tan\beta$, when the enhancement of the $ht\bar{t}$ coupling becomes small, $R^{\rm VBF/VH}_{\gamma\gamma}$ becomes bigger than $R^{\rm tth}_{VV}$. This happens for $\tan\beta \gtrsim 2.5$, as can be seen from figure 3.

A preference for low $\tan\beta$ is emphasized in figure 3. It can be seen that for $1 \lesssim \tan\beta \lesssim 1.5$, $R^{\rm tth}_{VV}$ can exceed 2.5, while keeping other rates within $2\sigma$ from the corresponding



JHEP05(2016)123

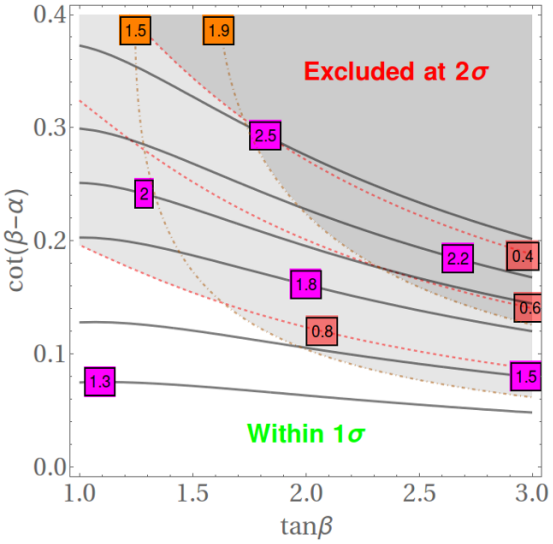


**Figure 3**. Contour plot of $R^{\rm tth}_{VV}$ (black solid lines with magenta labels), $R^{\rm VBF/VH}_{\tau\tau}$ (dashed red lines with red labels) and $R^{\rm VBF/VH}_{\gamma\gamma}$ (dot-dashed orange lines with orange labels) in the plane ($\tan\beta$, $\cot(\beta-\alpha)$) in type-II 2HDM with light stops. Darker grey region is excluded at $2\sigma$ by at least one channel, while in the white region all the rates are within $1\sigma$ from the corresponding central values. The value of the gluon fusion rates can be always adjusted by a proper choice of parameters in the stop sector. In order to calculate the total decay width $\delta c_g = -0.25$ is used in this plot, which is a typical value needed to keep the gluon fusion rates close to the SM values when $tth$ rates are enhanced, while $\delta c_\gamma = 2\delta c_g/9$. The position of the contours vary rather mildly with $\delta c_g$.

experimental central values. In order to keep all the rates within $1\sigma$, $R^{\rm VBF/VH}_{\tau\tau}$ must be above about 0.8 which for $\tan\beta = 1$ allows for $R^{\rm tth}_{VV}$ up to about 1.8.

It is interesting to note that maximal value of $R^{\rm tth}_{VV}$, consistent with other data at $2\sigma$, decreases quite slowly with $\tan\beta$. The reason is that the branching ratio of the Higgs decaying to $VV$ increases with $\tan\beta$ which partly compensates the decrease of $\sigma^{\rm tth}$. Keeping all the rates within $2\sigma$ from the corresponding experimental central values, $R^{\rm tth}_{VV} = 2$ is possible as long as $\tan\beta \lesssim 2.5$, even if $R^{\rm VBF/VH}_{\tau\tau} \geq 0.6$ is taken, which seems to be more realistic than allowing values as low as 0.4 for this quantity.

Let us end this section with a comment that in generic supersymmetric extensions of the SM there is a correlation between the Higgs couplings and the Higgs mass so typically one expect additional constraints on possible $tth$ enhancement imposed by the Higgs mass measurement of 125 GeV. Moreover, light highly-mixed stops required to keep the gluon fusion rate under control may induce non-negligible loop corrections to the off-diagonal entry of the Higgs mass matrix, hence also to the Higgs couplings, especially if the second Higgs doublet is light. In particular, this is the case for NMSSM which we discuss in detail in the next section.

## 4 tth in the NMSSM

Let us now discuss $tth$ production in NMSSM which is a more restrictive framework because the mixing angles in the Higgs sector are functions of NMSSM parameters which cannot



JHEP05(2016)123

| | B1 | B2 | B3 |
|---|---|---|---|
| $\tan\beta$ | 1 | 1.5 | 2 |
| $\cot(\beta-\alpha)$ | 0.25 | 0.22 | 0.18 |
| $m_{\tilde{t}_1}$ | 200 | 200 | 210 |
| $m_{\tilde{t}_2}$ | 700 | 700 | 700 |
| $\tilde{X}_t/m_{\tilde{t}_2}$ | 1.7 | 1.6 | 1.6 |
| $R_{VV}^{\rm tth}$ | 2.02 | 1.96 | 1.90 |
| $R_{\gamma\gamma}^{\rm tth}$ | 2.09 | 2.09 | 2.07 |
| $R_{VV}^{\rm gg}$ | 1.18 | 1.21 | 1.19 |
| $R_{\gamma\gamma}^{\rm gg}$ | 1.22 | 1.29 | 1.29 |
| $R_{VV}^{\rm VBF/VH}$ | 1.29 | 1.49 | 1.60 |
| $R_{\gamma\gamma}^{\rm VBF/VH}$ | 1.33 | 1.59 | 1.74 |
| $R_{\tau\tau}^{\rm VBF/VH}$ | 0.73 | 0.67 | 0.66 |

**Table 2**. List of benchmark points for Type-II 2HDM with light stops. All masses are in GeV.

take arbitrary values. We focus on the general NMSSM for which the MSSM superpotential is supplemented by (we use the notation of ref. [21]):

$$W_{\rm NMSSM} = \lambda S H_u H_d + f(S)\,. \tag{4.1}$$

The first term is the source of the effective higgsino mass parameter, $\mu_{\rm eff} \equiv \lambda v_s$ (we drop the subscript "eff" in the rest of the paper), while the second term parametrizes various versions of NMSSM. In the simplest version, known as the scale-invariant NMSSM, $f(S) \equiv \kappa S^3/3$, while in more general models $f(S) \equiv \xi_F S + \mu' S^2/2 + \kappa S^3/3$.

It is more convenient for us to work in the Higgs basis $(\hat{h}, \hat{H}, \hat{s})$, where $\hat{h} = H_d \cos\beta + H_u \sin\beta$, $\hat{H} = H_d \sin\beta - H_u \cos\beta$ and $\hat{s} = S$. This is because $\hat{h}$ field has exactly the same couplings to the gauge bosons and fermions as the SM Higgs field. The field $\hat{H}$ does not couple to the gauge bosons and its couplings to the up and down fermions are the SM Higgs ones rescaled by $\tan\beta$ and $-\cot\beta$, respectively. The mass eigenstates are denoted as $s$, $h$, $H$, with the understanding that $h$ is the SM-like Higgs.

In the hatted basis the tree-level Higgs mass matrix in general NMSSM is given by:

$$\hat{M}^2 = \begin{pmatrix} \hat{M}^2_{hh} & \hat{M}^2_{hH} & \hat{M}^2_{hs} \\ \hat{M}^2_{hH} & \hat{M}^2_{HH} & \hat{M}^2_{Hs} \\ \hat{M}^2_{hs} & \hat{M}^2_{Hs} & \hat{M}^2_{ss} \end{pmatrix}, \tag{4.2}$$

where, at tree level,

$$\hat{M}^2_{hh} = M_Z^2 \cos^2(2\beta) + \lambda^2 v^2 \sin^2(2\beta)\,, \tag{4.3}$$

$$\hat{M}^2_{HH} = (M_Z^2 - \lambda^2 v^2)\sin^2(2\beta) + \frac{2B\mu}{\sin(2\beta)}\,, \tag{4.4}$$

$$\hat{M}^2_{ss} = \frac{1}{2}\lambda v^2 \sin 2\beta \left(\frac{\Lambda}{v_s} - \langle \partial_S^3 f\rangle\right) + \Upsilon\,, \tag{4.5}$$

$$\hat{M}^2_{hH} = \frac{1}{2}(M_Z^2 - \lambda^2 v^2)\sin 4\beta\,, \tag{4.6}$$

$$\hat{M}^2_{hs} = \lambda v(2\mu - \Lambda \sin 2\beta)\,, \tag{4.7}$$

$$\hat{M}^2_{Hs} = \lambda v \Lambda \cos 2\beta\,. \tag{4.8}$$

where $\Lambda \equiv A_\lambda + \langle \partial_S^2 f\rangle$, $B \equiv A_\lambda + \langle \partial_S f\rangle/v_s + m_3^2/(\lambda v_s)$, $\Upsilon \equiv \langle (\partial_S^2 f)^2\rangle + \langle \partial_S f \partial_S^3 f\rangle - \frac{\langle \partial_S f \partial_S^2 f\rangle}{v_s} + A_\kappa \kappa v_s - \frac{\xi_S}{v_s}$ and $v \approx 174\,\mathrm{GeV}$.

Since we are mainly interested in the enhancement of the $tth$ production cross-section small mixing between the Higgs $h$ and the singlet is preferred. Since the main effects come from admixture of the $h$ and $H$, we assume that the singlet components of $h$ and $H$ are negligible, which can be obtained by taking appropriately large $\hat{M}^2_{ss}$. Nevertheless, even with approximately decoupled singlet NMSSM is very different from MSSM because of the Higgs-singlet interaction controlled by the coupling $\lambda$. For instance, as was discussed in ref. [22, 23] the mixing between $h$ and $H$ take small values for $\lambda \simeq 0.6$–$0.7$, leading to an effective alignment of the SM-like Higgs bosons for these values of the trilinear couplings.

These properties may be easily understood by studying the CP-even Higgs mass matrix properties. For values of $\tan\beta$ of order one, the dominant loop correction contributes to $M^2_{H_u H_u}$ entry but after the rotation to the Higgs basis gives also correction to the diagonal and off-diagonal entries of the CP-even Higgs mass matrix (for the approximate expression of these corrections, see, for instance, ref. [22, 23]). We shall parametrize these corrections by those affecting the $hh$ matrix element,

$$\hat{M}^2_{hh} = M_Z^2 \cos^2(2\beta) + \lambda^2 v^2 \sin^2(2\beta) + \Delta^2_{\rm loop} \tag{4.9}$$

It is straightforward to show that in this case

$$\cot(\beta - \alpha) = \frac{\frac{1}{2}(M_Z^2 - \lambda^2 v^2)\sin 4\beta - \Delta^2_{\rm loop}/\tan\beta}{\hat{M}^2_{HH} - m_h^2} \tag{4.10}$$

where we used the notation of the 2HDM which is justified as long as the singlet admixture in $h$ and $H$ is negligible. The enhancement of $R^{\rm tth}_{VV}$ requires $\cot(\beta - \alpha) > 0$ which implies $(M_Z^2 - \lambda^2 v^2)\sin 4\beta > 0$ for $m_H > m_h$ when $\Delta_{\rm loop}$ is neglected. Note that, at tree level for $\tan\beta = 1$, $\cot(\beta - \alpha) = 0$ and the enhancement of the $ht\bar{t}$ coupling requires $\lambda v > (<) M_Z$ for $\tan\beta > (<) 1$. This implies that $\tan\beta < 1$ is disfavoured because the $tth$ enhancement is possible only if the tree-level Higgs mass is smaller than in MSSM with large $\tan\beta$, so (at least) one stop would have to be very heavy in order to account for the 125 GeV Higgs. Moreover, for $\tan\beta < 1$ the top Yukawa coupling enters the non-perturbative regime close to the TeV scale.

Notice also that $\Delta_{\rm loop}$, which is dominated by stop loops, is positive[2] so after taking into account loop effects, for $\tan\beta > 1$, the critical value of $\lambda$, above which the $tth$ cross-section is enhanced, is larger than $M_Z/v$. This may be easily understood by rewriting the

[2]Negative $\Delta_{\rm loop}$ is possible only for very large stop mixing which would lead to destabilization of the EW vacuum [24–26].



JHEP05(2016)123

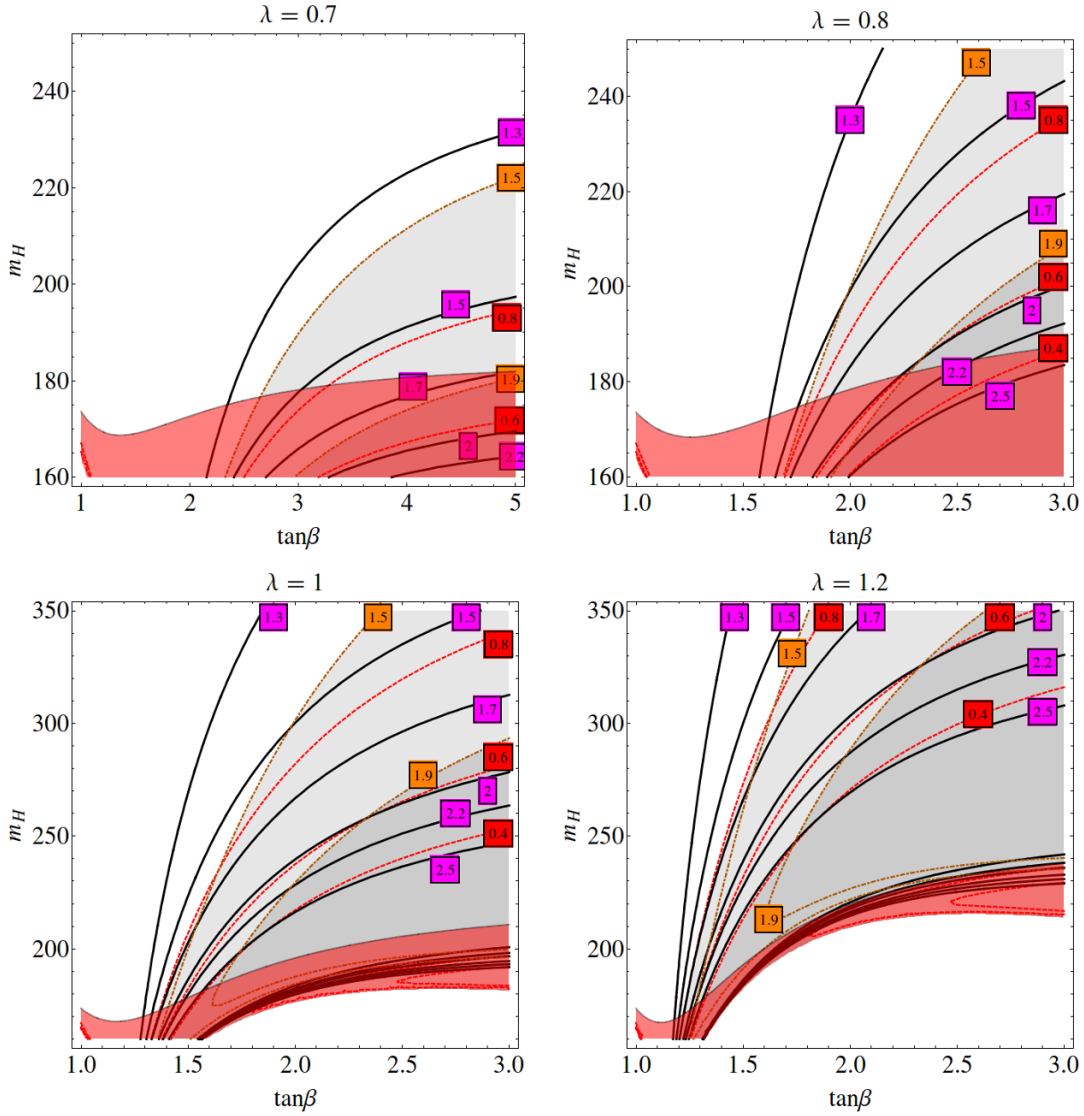


**Figure 4**. The same as in figure 3 but for NMSSM in the $(\tan\beta\text{-}m_H)$ plane for several values of $\lambda$ using the approximate formula (4.10) with $\Delta_{\rm loop} = 75\,\text{GeV}$. The red shaded area is excluded because $m_{H^\pm} < 160\,\text{GeV}$ there. The white area below the red shaded area (visible in the lower panels) is theoretically inaccessible for $m_h = 125\,\text{GeV}$.

expression of $\cot(\beta-\alpha)$ in terms of the $\hat{M}^2_{hh}$ matrix element, namely

$$\cot(\beta-\alpha) = -\frac{\hat{M}^2_{hh} - \cos(2\beta)M_Z^2 - 2\lambda^2 v^2 \sin^2(\beta)}{\tan\beta\left(\hat{M}^2_{HH} - m_h^2\right)} \tag{4.11}$$

Since $\hat{M}^2_{hh} \simeq m_h^2$, one can easily show that for $\tan\beta = \mathcal{O}(1)$ the lightest Higgs alignment, for which $\cot(\beta-\alpha) \simeq 0$, occur for values of $\lambda$ in the range $\lambda \simeq 0.65$–$0.7$ [22, 23], with larger values of $\lambda$ leading to positive values of $\cot(\beta-\alpha)$ and hence to an enhancement of the top quark coupling to $h$.



JHEP05(2016)123

In the rest of the presentation we fix $\Delta_{\rm loop} = 75\,\text{GeV}$ which is a typical value of the loop correction for the stop masses in the range of several hundreds GeV and large stop mixing. We checked that such value of $\Delta_{\rm loop}$ for $\tan\beta \approx 2$ leads to the results that are in a good agreement with a more precise calculation by `NMSSMTools 4.8.1` (that diagonalizes the full loop corrected 3x3 NMSSM Higgs mass matrix) [27, 28] that shows that $\lambda \gtrsim 0.6$ is required for the $tth$ enhancement. One technical comment is that we choose to fix $\Delta_{\rm loop}$ rather than adjust $\Delta_{\rm loop}$ to get the Higgs mass of 125 GeV. This is because for large $\lambda$ that would require negative values of $\Delta_{\rm loop}$ which cannot be obtained if the vacuum stability constraints are taken into account. We assume, instead, that the Higgs mass is set to 125 GeV by mixing effects with the heavy singlet [29]. Indeed, it can be shown that the mixing with the singlet can give large negative correction to $m_h$ even if this mixing changes the Higgs couplings in a negligible amount [21].

In figure 4 contours of $R^{\rm tth}_{VV}$ in the plane ($\tan\beta$,$m_H$) for several values of $\lambda$ are presented. In these plots $m_h$ is fixed to 125 GeV and the Higgs couplings that enter the formulae for cross-sections and branching ratios are determined by eq. (4.10). Notice that, in contrast to a general type-II 2HDM discussed in the previous section, values of $\tan\beta$ as small as possible are no longer preffered. This is because in NMSSM $\cot(\beta-\alpha)$ is not independent from $\tan\beta$ and as stressed above it actually vanishes at tree level in the limit $\tan\beta \to 1$. In fact, enhancement of the $ht\bar{t}$ coupling (with respect to the Higgs coupling to massive gauge bosons) is maximized for $\tan\beta \approx 2$. $R^{\rm tth}_{VV}$ is maximized for even larger $\tan\beta$ due to larger suppression of the $hb\bar{b}$ coupling but as discussed above the latter possibility is constrained by the LHC data in other channels. Therefore, after taking into account the experimental constraints $R^{\rm tth}_{VV}$ is typically maximal for $\tan\beta$ close to 2.

It can be also seen that if one demands perturbativity up to the GUT scale, which for small $\tan\beta$ can be realised only for $\lambda \lesssim 0.7$, substantial enhancement of $\sigma^{\rm tth}$ with respect to $\sigma^{\rm VBF/VH}$ is possible only for very light $H$. This is a consequence of the approximate alignment in the NMSSM Higgs sector for $\lambda \sim 0.6$ [22, 23]. However, the region of light $H$ is strongly constrained, because the CP-odd and charged Higgses are also light in such a case. At tree level:

$$m_A^2 = \hat{M}_{HH}^2 - (M_Z^2 - \lambda^2 v^2)\sin^2(2\beta)\,, \tag{4.12}$$

$$m_{H^\pm}^2 = m_A^2 + m_W^2 - \lambda^2 v^2\,. \tag{4.13}$$

In the context of the MSSM, the constraints on light BSM Higgses were studied e.g. in ref. [30]. However, the Higgs sector of NMSSM with large $\lambda$ is significantly different from that of MSSM. Very important constraint comes from the charged Higgs searches. Particularly important search is in the channel $t \to H^+ b$ ($H^+ \to \tau^+\nu_\tau$) which for most values of $\tan\beta$ excludes $m_{H^\pm} < 160\,\text{GeV}$ both by ATLAS [31] and CMS [32]. Slightly weaker bounds on $m_{H^\pm}$ have been found for $\tan\beta$ in the range between 4 and 20 which has no big impact on our results since the $tth$ enhancement prefers lower values of $\tan\beta$. As can be seen from figure 4, this search excludes the smallest values of $m_H$ and the exclusion becomes stronger as $\lambda$ grows as a consequence of relations (4.12)–(4.13). After taking this constraint into account the $ht\bar{t}$ coupling cannot be significantly enhanced for values of $\lambda$



JHEP05(2016)123

consistent with the perturbativity up to the GUT scale. In such a case $R^{\rm tth}_{VV}$ can only be enhanced as a result of the suppression of the $hb\bar{b}$ coupling, that occurs at larger $\tan\beta$. For larger $\tan\beta$ perturbativity constraint on $\lambda$ becomes slightly weaker and can be satisifed e.g. for $\lambda = 0.76$ and $\tan\beta = 4$. Such a case is represented by point P1 in table 3 which consists a list of benchmarks obtained with `NMSSMTools`. One can see that $R^{\rm VBF/VH}_{\gamma\gamma}$ for such $\tan\beta$ is always larger than $R^{\rm tth}_{VV}$ and provides the main constraint for the latter.

Relaxing the requirement of perturbativity up to the GUT scale, substantial enhancement of the $ht\bar{t}$ coupling becomes possible resulting in $R^{\rm tth}_{VV} \approx 2$ without violating constraints from other Higgs signal strengths, as long as $\tan\beta$ is close to 2. Already for $\lambda \approx 0.8$ and $\tan\beta \approx 2$, $R^{\rm tth}_{VV} \approx 2$ can be obtained with $m_{H^\pm} > 160\,\text{GeV}$. However, there are additional constraints coming from the LHC searches for the CP-even Higgs in the $ZZ$ and $WW$ decay channels [34]–[39] and searches for the CP-odd Higgs in the $\tau\tau$ [40, 41] and $hZ$ [42, 43] decay channels. Points with $R^{\rm tth}_{VV} \approx 2$ typically violate some of those constraints, especially the constraint from the $H \to ZZ$ searches, unless $H$ and $A$ have significant fraction of invisible decays. Therefore, valid points with large $tth$ enhancement must have light neutralino (but not lighter than $m_h/2$ to avoid invisible $h$ decays). Light neutralino is preferred also in order to avoid the LHC constraints on light stop. Indeed, keeping the gluon fusion rates in the gauge boson decay channels close to the SM prediction when $R^{\rm tth}_{VV}$ is enhanced requires the lightest stop mass to be below about 300 GeV.[3] Such a light stop is excluded by the ATLAS [44]–[47] and CMS [48]–[51] stop searches unless the mass splitting between the stop and the LSP is very close to the top mass, $W$ mass or zero. Moreover, for the stop mass below about 250 GeV the zero mass splitting between the stop and the LSP is excluded by the CMS monojet search [50]. Therefore, generically if the light stop is consistent with the LHC data then some of the decays of the heavy Higgses are invisible. In the NMSSM with enhanced $tth$ rates, the best candidate for the LSP is singlino-like neutralino because due to the mixing with Higgsinos and the large values of $\lambda$, the decay width of heavy Higgses to singlino is typically large (if kinematically accessible).

Points P2, P3 and P4 in table 3 are the NMSSM points that have a Landau pole below the GUT scale and were obtained with `NMSSMTools` and satisfy all experimental constraints on the Higgs sector, which was verified with `HiggsBounds 4.2.1` [33]. Constraints on the light stop are also satisfied because the mass splitting between the stop and the LSP is very close to the top mass. All the benchmark points predict $R^{\rm tth}_{VV} \approx 2$. Benchmark P2 is characterized by $\lambda = 0.85$ and $\tan\beta = 2$ and $m_{H^\pm}$ just above 160 GeV. For smaller values of $\lambda$ and $\tan\beta = 2$ we have not found points with $R^{\rm tth}_{VV} \approx 2$ that are consistent simultanously with the LHC $H \to WW$ and $H \to ZZ$ searches. The crucial role for the benchmark P2 to be consistent with the Higgs data is played by large branching ratios of $A$ and $H$ decays to pairs of LSP.

Benchmark P3 with $\lambda = 1.1$ and $\tan\beta = 2$ is characterized by $m_H$ above 2 $m_h$ and the main role in avoiding constraints from the $H \to ZZ$ searches is played by large BR(H $\to$ hh) but invisible decays are needed to avoid the constraints from $A \to hZ$ searches. For even

[3] For larger $m_{\tilde{t}_1}$ the stop correction to the effective Higgs coupling to gluons (3.1) is too small unless $\tilde{X}_t/m_{\tilde{t}_2}$ is so large that the EW vacuum becomes unstable.



JHEP05(2016)123

| | P1 | P2 | P3 | P4 | P5 |
|---|---|---|---|---|---|
| $\lambda$ | 0.76 | 0.85 | 1.1 | 1.4 | 1.4 |
| $\tan\beta$ | 4 | 2 | 2 | 1.5 | 1.5 |
| $m_{Q_3}$ | 700 | 700 | 700 | 700 | 700 |
| $m_{U_3}$ | 500 | 480 | 500 | 480 | 450 |
| $A_t$ | -1170 | -1100 | -1030 | -780 | -1030 |
| $\mu$ | 300 | 770 | 1040 | 1060 | 390 |
| $M_2$ | 500 | 500 | 500 | 500 | -90 |
| $\mu'$ | 60 | 45 | 40 | 14 | -24 |
| $M_{P_1}$ | 193 | 197 | 277 | 332 | 357 |
| $M_{P_2}$ | 2000 | 2500 | 3000 | 2400 | 800 |
| $m_h$ | 125.1 | 125.9 | 125.0 | 124.9 | 125.0 |
| $m_H$ | 192 | 184 | 262 | 280 | 299 |
| $m_{H^\pm}$ | 167 | 161 | 236 | 257 | 272 |
| $m_A$ | 195 | 204 | 293 | 342 | 344 |
| $m_{\tilde{\chi}_1^0}$ | 70 | 65 | 66 | 63 | 89 |
| $m_{\tilde{\chi}_1^\pm}$ | 282 | 504 | 516 | 514 | 109 |
| $m_{\tilde{t}_1}$ | 236 | 232 | 241 | 231 | 222 |
| $m_{\tilde{t}_2}$ | 726 | 752 | 766 | 757 | 730 |
| $R_{VV}^{\mathrm{tth}}$ | 1.79 | 1.84 | 1.96 | 1.92 | 1.87 |
| $R_{\gamma\gamma}^{\mathrm{tth}}$ | 1.97 | 2.12 | 2.22 | 2.19 | 1.96 |
| $R_{VV}^{\mathrm{gg}}$ | 1.16 | 1.00 | 1.12 | 1.18 | 1.23 |
| $R_{\gamma\gamma}^{\mathrm{gg}}$ | 1.29 | 1.15 | 1.27 | 1.34 | 1.29 |
| $R_{VV}^{\mathrm{VBF/VH}}$ | 1.70 | 1.57 | 1.65 | 1.48 | 1.43 |
| $R_{\gamma\gamma}^{\mathrm{VBF/VH}}$ | 1.89 | 1.80 | 1.87 | 1.69 | 1.50 |
| $R_{\tau\tau}^{\mathrm{VBF/VH}}$ | 0.70 | 0.71 | 0.67 | 0.71 | 0.65 |
| $\mathrm{BR}(H \to \tilde{\chi}_1^0\tilde{\chi}_1^0)$ | 0.71 | 0.49 | 0.24 | 0.14 | 0.19 |
| $\mathrm{BR}(H \to \tilde{\chi}_1^0\tilde{\chi}_2^0)$ | 0 | 0 | 0 | 0 | 0.17 |
| $\mathrm{BR}(H \to hh)$ | 0 | 0 | 0.47 | 0.71 | 0.54 |
| $\mathrm{BR}(A \to \tilde{\chi}_1^0\tilde{\chi}_1^0)$ | 0.85 | 0.89 | 0.78 | 0.75 | 0.88 |
| $\mathrm{BR}(A \to H^\pm W^\mp)$ | 0 | 0 | 0 | 0.05 | 0 |

**Table 3**. List of benchmark points obtained with `NMSSMTools 4.8.1`. All masses are in GeV. All points satisfy all experimental constraints from the Higgs signal strength measurements, as well as from direct searches for Higgses, checked with `HiggsBounds 4.2.1` [33], and stops. The remaining soft sfermion masses are set to 2 TeV, $M_3 = 1.5$ TeV, $M_1 = 250$ GeV. All the remaining $A$-terms are set to 1.5 TeV, while $\kappa = A_\kappa = 0$. The remaining parameters are calculated with `NMSSMTools` using EWSB conditions and the values of $\mu$ and $M_{P_i}$ (with $M_{P_i}$ defined as the diagonal entries of the pseudoscalar mass matrix). The above spectra were obtained with the renormalization scale set to 700 GeV.



JHEP05(2016)123

larger values of $\lambda$, $R_{VV}^{\rm tth} \approx 2$ can be obtained also for $\tan\beta$ significantly below 2. Such a case is represented by benchmark P4 with $\lambda = 1.4$ and $\tan\beta = 1.5$. Notice that in this case $R_{VV}^{\rm tth}$ is similar to other benchmarks but the VBF rates are smaller than for $\tan\beta = 2$. Note also that for such a large $\lambda$ the splitting between the charged Higgs mass and CP-odd Higgs mass is so large that decays of the latter to the charged Higgs and W boson become kinematically accessible which additionally helps in satisfying the constraints from $A \to hZ$ searches.

It should be noted that $R_{VV}^{\rm tth}$ of about 2 in the NMSSM typically ruins the $1\sigma$ agreement with the combined VBF measurements in the $\gamma\gamma$ decay channel because although CMS observed an enhancement, ATLAS observed some suppression (with respect to the SM prediction) in this channel. This feature is specific to NMSSM and results from the approach to alignment in the limit $\tan\beta \to 1$. As emphasized before, in general type-II 2HDM (with new colored states that keep the gluon fusion production rate close to the SM prediction) $R_{VV}^{\rm tth}$ of about 2 is possible without large modifications to the VBF rates provided that $\tan\beta \approx 1$, cf. benchmark B1 in table 2.

Nevertheless, strongly enhanced $R_{VV}^{\rm tth}$ without violating $1\sigma$ agreement with the combined VBF measurements in the $\gamma\gamma$ decay channel can also be obtained in the NMSSM provided that a chargino is very light and $\mathrm{sgn}(\mu M_2) < 0$. In such a case the chargino loop contribution to the $\gamma\gamma$ decay rate interferes destructively with the dominant W boson loop. In order to substantially alter the $\gamma\gamma$ rate the lightest chargino should be not far above 100 GeV, which is a generic lower mass limit for chargino from LEP [52], with non-negligible mixing between higgsino and gaugino component [53, 54].[4] This effect is demonstrated by benchmark P5 in table 3 where $R_{VV}^{\rm tth}$ of about 1.9 is obtained with $R_{\gamma\gamma}^{\rm VBF/VH} \approx 1.5$. For benchmark P5, the stop collider phenomenology differs from other benchmarks because the lightest stop can decay to the lightest chargino and a bottom quark. In such a case limits for direct stop production typically become stronger, but some parts of parameter space with light stop are still allowed. For example, a stop with mass of 220 GeV decaying to a chargino and a bottom quark in the case of a 20 GeV mass splitting between the chargino and the LSP, with the LSP mass around 90 GeV, as it is the case for benchmark P5, is consistent with the LHC data [44, 47, 48]. Due to the presence of a light wino-dominated chargino in benchmark 5, limits for direct wino-like $\tilde{\chi}_1^\pm - \tilde{\chi}_2^0$ production may also be relevant. In this case, $\tilde{\chi}_1^\pm$ decays to a W boson and the LSP and the mass limits for $\tilde{\chi}_1^\pm$ (assumed to be degenerate with $\tilde{\chi}_2^0$) depend on the decay pattern of $\tilde{\chi}_2^0$. For benchmark 5, $\tilde{\chi}_2^0$ decays to the LSP and a photon or off-shell $Z$ boson with $\mathrm{BR}(\tilde{\chi}_2^0 \to \tilde{\chi}_1^0\gamma) \approx 55\%$. For both decay patterns the LHC searches are not yet sensitive for such a small mass splitting between the chargino and the LSP [57–59].

Let us also comment on the fact that benchmark points P2-P5 in table 3 are in conflict with B-physics constraints if minimal flavour violation (MFV) is assumed. In particular $\mathrm{BR}(b \to s\gamma)$ is typically about $5 \cdot 10^{-4}$ which is somewhat above the experimental value [60]. This tension originates from large loop contributions from light highly-mixed

[4] For large $\lambda$ the $\gamma\gamma$ rate can be also modified if higgsino-dominated chargino is light and the Higgs has a non-negligible singlet component [55, 56].



JHEP05(2016)123

stops and the charged Higgs. Nevertheless, BR($b \to s\gamma$) can be brought in agreement with the experimental data by arranging parameters such that the charged Higgs contribution to BR($b \to s\gamma$) is approximately canceled by the corresponding stop contribution. One should also keep in mind that B-physics observables are sensitive to flavour structure of the down squark parameters via loops with gluinos so they can be brought in agreement with measurements by adjusting non-MFV parameters [61].

## 5 Conclusions

We have investigated enhancement of the $tth$ production cross-section in models with the Higgs sector that can be approximately described as type-II 2HDM. We have shown that in this class of models the $tth$ signal rates in the gauge boson decay channels can be more than two times larger than in the SM, as hinted by the ATLAS and CMS excesses, provided that $\tan\beta$ is small and additional light colored particles, such as the stop, interfere destructively with the top quark in the gluon fusion amplitude. In these models, the necessary decrease of the top quark coupling to the lightest Higgs is associated with a reduction of the bottom quark coupling, which contributes to an enhancement of the Higgs decay into gauge bosons.

We have also shown that large $tth$ enhancement of about two can be realized in the NMSSM, although the situation is more constrained in this case, due to the specific dependence of the CP-even Higgs matrix elements on the model parameters. For instance, this requires values of $\lambda$ larger than the ones allowing the perturbative consistency of the theory up to the GUT scale. Moreover, $\tan\beta$ must be above one (preferably between 1.5 and 2), what implies a sizable reduction of the bottom coupling to the lightest Higgs boson and hence a large enhancement of the decays of the lightest CP-even Higgs into gauge bosons. It should be noted that the NMSSM realization of $tth$ enhancement is not generic and requires some tuning in the stop sector to keep the gluon fusion rates close to the SM prediction. Moreover, since this scenario points to large values of $\lambda$ and small $\tan\beta$ the Higgs mass generically turns out to be too large but can be set to 125 GeV by introducing small amount of mixing between the Higgs and the singlet scalar which partially cancels large contribution to the Higgs mass proportional to $\lambda$.

If the $tth$ excess persists in the LHC run 2 data, the NMSSM interpretation of it can be tested at the LHC in multiple ways. First of all, since signal rates in VBF production channel show correlated deviations with the $tth$ signal rates, improved measurements of the VBF production mode, especially in the $\gamma\gamma$ decay channel, can set strong constraints on this scenario. Secondly, the gluon fusion signal strengths are close to the SM prediction due to the presence of a light stop with mass below 300 GeV, which is consistent with current LHC searches because its mass splitting with the LSP is close to the top quark mass, or because there is an additional light chargino with mass close to 100 GeV and a few tens of GeV heavier than the LSP. Therefore, direct stop (and in some scenarios chargino) searches in this region of parameters can also efficiently probe this model. Light stop contribution to the gluon fusion cross-section can be also probed by looking for a boosted Higgs with a jet [10]. Finally, this scenario can be tested at the LHC by direct searches of MSSM-like Higgs bosons which masses have to be in the range of several hundred of GeV to allow for substantial $tth$ enhancement.



JHEP05(2016)123

## Acknowledgments

This work has been partially supported by National Science Centre under research grant DEC-2014/15/B/ST2/02157. MB acknowledges support from the Polish Ministry of Science and Higher Education (decision no. 1266/MOB/IV/2015/0). Work at ANL is supported in part by the U.S. Department of Energy, Office of High Energy Physics, under Contract No. DE-AC02-06CH11357. Work at the University of Chicago is supported in part by U.S. Department of Energy grant number DE-FG02-13ER41958. MB would like to thank Cyril Hugonie, Ulrich Ellwanger and Tim Stefaniak for useful correspondence about `NMSSMTools` and `HiggsBounds`. MB thanks the Galileo Galilei Institute for Theoretical Physics and INFN for hospitality and partial support during the completion of this work. C.W thanks the hospitality of the Aspen Center for Physics, which is supported by the National Science Foundation under Grant No. PHYS-1066293.

## A Higgs signal rate computation

In the computation of cross-sections and branching ratios normalized to the SM values we use the formalism of ref. [18]. In 2HDM, deviations from the SM predictions occur through the modifications of the Yukawa coupling to up-type fermions, $c_t$, the Yukawa coupling to down-type fermions, $c_b$, and the couplings to $W$ and $Z$ bosons, $c_V$, which are normalised to the SM values. Using these normalised couplings the most relevant Higgs decay widths are given by:

$$\Gamma(h \to VV) = c_V^2 \Gamma(h \to VV)^{\rm SM}\,, \tag{A.1}$$

$$\Gamma(h \to bb/\tau\tau) = c_b^2 \Gamma(h \to bb/\tau\tau)^{\rm SM}\,, \tag{A.2}$$

$$\Gamma(h \to cc) = c_t^2 \Gamma(h \to cc)^{\rm SM}\,, \tag{A.3}$$

$$\Gamma(h \to gg) = \left|\frac{\hat{c}_g}{\hat{c}_g^{\rm SM}}\right|^2 \Gamma(h \to gg)^{\rm SM}\,, \tag{A.4}$$

$$\Gamma(h \to \gamma\gamma) = \left|\frac{\hat{c}_\gamma}{\hat{c}_\gamma^{\rm SM}}\right|^2 \Gamma(h \to gg)^{\rm SM}\,. \tag{A.5}$$

The decays to gluons and photons are loop-induced and the leading contribution to these decays can be described by dimension-5 operators with $\hat{c}_g$ and $\hat{c}_\gamma$ being the corresponding effective Higgs couplings to gluons and photons, respectively, which are approximately given by:

$$\hat{c}_g = c_g + (-0.06 + 0.09i)c_b\,, \qquad \hat{c}_\gamma = c_\gamma - 1.04 c_V\,. \tag{A.6}$$

The SM values of $c_g$ and $c_\gamma$, which arise from integrating out a top quark, are approximately given by:

$$c_g^{\rm SM} \approx 1.03\,, \tag{A.7}$$

$$c_\gamma^{\rm SM} \approx \frac{2}{9}\,1.03\,. \tag{A.8}$$

Beyond the SM, $c_g$ and $c_\gamma$ are given by:

$$c_g = c_g^{\rm SM} c_t + \delta c_g \,, \tag{A.9}$$

$$c_\gamma = c_\gamma^{\rm SM} c_t + \delta c_\gamma \,. \tag{A.10}$$

where $\delta c_i$ stand for the contributions from new particles that couple to the Higgs.

The production cross-sections scale like:

$$\sigma^{tth} \equiv \frac{\sigma(gg \to tth)}{\sigma^{\rm SM}(gg \to tth)} = c_t^2 \,, \tag{A.11}$$

$$\sigma^{gg} \equiv \frac{\sigma(gg \to h)}{\sigma^{\rm SM}(gg \to h)} = \left| \frac{\hat{c}_g}{\hat{c}_g^{\rm SM}} \right|^2 \,, \tag{A.12}$$

$$\sigma^{\rm VBF} \equiv \frac{\sigma(q\bar{q} \to hjj)}{\sigma^{\rm SM}(q\bar{q} \to hjj)} = \sigma^{VH} \equiv \frac{\sigma(q\bar{q} \to hV)}{\sigma^{\rm SM}(q\bar{q} \to hV)} = c_V^2 \,, \tag{A.13}$$

$$\tag{A.14}$$



## References

[1] ATLAS collaboration, *Observation of a new particle in the search for the standard model Higgs boson with the ATLAS detector at the LHC*, *Phys. Lett.* **B 716** (2012) 1 [arXiv:1207.7214] [INSPIRE].

[2] CMS collaboration, *Observation of a new boson at a mass of* 125 *GeV with the CMS experiment at the LHC*, *Phys. Lett.* **B 716** (2012) 30 [arXiv:1207.7235] [INSPIRE].

[3] ATLAS and CMS Collaborations, *Measurements of the Higgs boson production and decay rates and constraints on its couplings from a combined ATLAS and CMS analysis of the LHC pp collision data at* $\sqrt{s} = 7$ *and* 8 *TeV*, ATLAS-CONF-2015-044 (2015) [CMS-PAS-HIG-15-002].

[4] C. Anastasiou et al., *High precision determination of the gluon fusion Higgs boson cross-section at the LHC*, *JHEP* **05** (2016) 058 [arXiv:1602.00695] [INSPIRE].

[5] D. de Florian and M. Grazzini, *Higgs production through gluon fusion: Updated cross sections at the Tevatron and the LHC*, *Phys. Lett.* **B 674** (2009) 291 [arXiv:0901.2427] [INSPIRE].

[6] S. Alioli, P. Nason, C. Oleari and E. Re, *NLO Higgs boson production via gluon fusion matched with shower in POWHEG*, *JHEP* **04** (2009) 002 [arXiv:0812.0578] [INSPIRE].

[7] C. Anastasiou, R. Boughezal and F. Petriello, *Mixed QCD-electroweak corrections to Higgs boson production in gluon fusion*, *JHEP* **04** (2009) 003 [arXiv:0811.3458] [INSPIRE].

[8] V. Ahrens, T. Becher, M. Neubert and L.L. Yang, *Renormalization-group improved prediction for Higgs production at hadron colliders*, *Eur. Phys. J.* **C 62** (2009) 333 [arXiv:0809.4283] [INSPIRE].

[9] A. Azatov and A. Paul, *Probing Higgs couplings with high* $p_T$ *Higgs production*, *JHEP* **01** (2014) 014 [arXiv:1309.5273] [INSPIRE].



JHEP05(2016)123

[10] C. Grojean, E. Salvioni, M. Schlaffer and A. Weiler, *Very boosted Higgs in gluon fusion*, *JHEP* **05** (2014) 022 [arXiv:1312.3317] [INSPIRE].

[11] ATLAS collaboration, *Search for the associated production of the Higgs boson with a top quark pair in multilepton final states with the ATLAS detector*, *Phys. Lett.* **B 749** (2015) 519 [arXiv:1506.05988] [INSPIRE].

[12] ATLAS collaboration, *Search for $H \to \gamma\gamma$ produced in association with top quarks and constraints on the Yukawa coupling between the top quark and the Higgs boson using data taken at 7 TeV and 8 TeV with the ATLAS detector*, *Phys. Lett.* **B 740** (2015) 222 [arXiv:1409.3122] [INSPIRE].

[13] CMS collaboration, *Search for the associated production of the Higgs boson with a top-quark pair*, *JHEP* **09** (2014) 087 [*Erratum ibid.* **1410** (2014) 106] [arXiv:1408.1682] [INSPIRE].

[14] P. Huang, A. Ismail, I. Low and C.E.M. Wagner, *Same-sign dilepton excesses and light top squarks*, *Phys. Rev.* **D 92** (2015) 075035 [arXiv:1507.01601] [INSPIRE].

[15] C.R. Chen, H.C. Cheng and I. Low, *Same-sign dilepton excesses and vector-like quarks*, *JHEP* **03** (2016) 098 [arXiv:1511.01452] [INSPIRE].

[16] A. Angelescu, A. Djouadi and G. Moreau, *Vector-like top/bottom quark partners and Higgs physics at the LHC*, *Eur. Phys. J.* **C 76** (2016) 99 [arXiv:1510.07527] [INSPIRE].

[17] U. Ellwanger, C. Hugonie and A.M. Teixeira, *The next-to-minimal supersymmetric standard model*, *Phys. Rept.* **496** (2010) 1 [arXiv:0910.1785] [INSPIRE].

[18] D. Carmi, A. Falkowski, E. Kuflik, T. Volansky and J. Zupan, *Higgs after the discovery: a status report*, *JHEP* **10** (2012) 196 [arXiv:1207.1718] [INSPIRE].

[19] A. Djouadi, *The anatomy of electro-weak symmetry breaking. II. The Higgs bosons in the minimal supersymmetric model*, *Phys. Rept.* **459** (2008) 1 [hep-ph/0503173] [INSPIRE].

[20] J.R. Espinosa, C. Grojean, V. Sanz and M. Trott, *NSUSY fits*, *JHEP* **12** (2012) 077 [arXiv:1207.7355] [INSPIRE].

[21] M. Badziak, M. Olechowski and S. Pokorski, *New regions in the NMSSM with a 125 GeV Higgs*, *JHEP* **06** (2013) 043 [arXiv:1304.5437] [INSPIRE].

[22] M. Carena, I. Low, N.R. Shah and C.E.M. Wagner, *Impersonating the standard model Higgs boson: alignment without decoupling*, *JHEP* **04** (2014) 015 [arXiv:1310.2248] [INSPIRE].

[23] M. Carena, H.E. Haber, I. Low, N.R. Shah and C.E.M. Wagner, *Alignment limit of the NMSSM Higgs sector*, *Phys. Rev.* **D 93** (2016) 035013 [arXiv:1510.09137] [INSPIRE].

[24] D. Chowdhury, R.M. Godbole, K.A. Mohan and S.K. Vempati, *Charge and color breaking constraints in MSSM after the Higgs discovery at LHC*, *JHEP* **02** (2014) 110 [arXiv:1310.1932] [INSPIRE].

[25] N. Blinov and D.E. Morrissey, *Vacuum stability and the MSSM Higgs mass*, *JHEP* **03** (2014) 106 [arXiv:1310.4174] [INSPIRE].

[26] J.E. Camargo-Molina, B. Garbrecht, B. O'Leary, W. Porod and F. Staub, *Constraining the natural MSSM through tunneling to color-breaking vacua at zero and non-zero temperature*, *Phys. Lett.* **B 737** (2014) 156 [arXiv:1405.7376] [INSPIRE].

[27] U. Ellwanger, J.F. Gunion and C. Hugonie, *NMHDECAY: a Fortran code for the Higgs masses, couplings and decay widths in the NMSSM*, *JHEP* **02** (2005) 066 [hep-ph/0406215] [INSPIRE].

[28] U. Ellwanger and C. Hugonie, *NMHDECAY 2.0: an updated program for sparticle masses, Higgs masses, couplings and decay widths in the NMSSM*, *Comput. Phys. Commun.* **175** (2006) 290 [hep-ph/0508022] [INSPIRE].



JHEP05(2016)123

[29] L.J. Hall, D. Pinner and J.T. Ruderman, *A natural SUSY Higgs near* 126 *GeV*, *JHEP* **04** (2012) 131 [arXiv:1112.2703] [INSPIRE].

[30] A. Djouadi, L. Maiani, A. Polosa, J. Quevillon and V. Riquer, *Fully covering the MSSM Higgs sector at the LHC*, *JHEP* **06** (2015) 168 [arXiv:1502.05653] [INSPIRE].

[31] ATLAS collaboration, *Search for charged Higgs bosons in the $\tau$+jets final state with pp collision data recorded at $\sqrt{s} = 8$ TeV with the ATLAS experiment*, ATLAS-CONF-2013-090 (2013).

[32] CMS collaboration, *Search for a charged Higgs boson in pp collisions at $\sqrt{s} = 8$ TeV*, *JHEP* **11** (2015) 018 [arXiv:1508.07774] [INSPIRE].

[33] P. Bechtle et al., *HiggsBounds-4: improved tests of extended Higgs sectors against exclusion bounds from LEP, the Tevatron and the LHC*, *Eur. Phys. J.* **C 74** (2014) 2693 [arXiv:1311.0055] [INSPIRE].

[34] ATLAS collaboration, *Search for a high-mass Higgs boson decaying to a W boson pair in pp collisions at $\sqrt{s} = 8$ TeV with the ATLAS detector*, *JHEP* **01** (2016) 032 [arXiv:1509.00389] [INSPIRE].

[35] ATLAS collaboration, *Observation and measurement of Higgs boson decays to $WW^*$ with the ATLAS detector*, *Phys. Rev.* **D 92** (2015) 012006 [arXiv:1412.2641] [INSPIRE].

[36] ATLAS collaboration, *Search for an additional, heavy Higgs boson in the $H \to ZZ$ decay channel at $\sqrt{s} = 8$ TeV in pp collision data with the ATLAS detector*, *Eur. Phys. J.* **C 76** (2016) 45 [arXiv:1507.05930].

[37] CMS collaboration, *Measurement of Higgs boson production and properties in the WW decay channel with leptonic final states*, *JHEP* **01** (2014) 096 [arXiv:1312.1129] [INSPIRE].

[38] CMS collaboration, *Measurement of the properties of a Higgs boson in the four-lepton final state*, *Phys. Rev.* **D 89** (2014) 092007 [arXiv:1312.5353] [INSPIRE].

[39] CMS collaboration, *Search for a Higgs boson in the mass range from* 145 *to* 1000 *GeV decaying to a Pair of W or Z bosons*, *JHEP* **10** (2015) 144 [arXiv:1504.00936] [INSPIRE].

[40] ATLAS collaboration, *Search for neutral Higgs bosons of the minimal supersymmetric standard model in pp collisions at $\sqrt{s} = 8$ TeV with the ATLAS detector*, *JHEP* **11** (2014) 056 [arXiv:1409.6064] [INSPIRE].

[41] CMS collaboration, *Search for neutral MSSM Higgs bosons decaying to a pair of tau leptons in pp collisions*, *JHEP* **10** (2014) 160 [arXiv:1408.3316] [INSPIRE].

[42] ATLAS collaboration, *Search for a CP-odd Higgs boson decaying to Zh in pp collisions at $\sqrt{s} = 8$ TeV with the ATLAS detector*, *Phys. Lett.* **B 744** (2015) 163 [arXiv:1502.04478] [INSPIRE].

[43] CMS collaboration, *Search for a pseudoscalar boson decaying into a Z boson and the* 125 *GeV Higgs boson in $\ell^+\ell^- b\bar{b}$ final states*, *Phys. Lett.* **B 748** (2015) 221 [arXiv:1504.04710] [INSPIRE].

[44] ATLAS collaboration, *Search for top squark pair production in final states with one isolated lepton, jets and missing transverse momentum in $\sqrt{s} = 8$ TeV pp collisions with the ATLAS detector*, *JHEP* **11** (2014) 118 [arXiv:1407.0583] [INSPIRE].

[45] ATLAS collaboration, *Search for pair-produced third-generation squarks decaying via charm quarks or in compressed supersymmetric scenarios in pp collisions at $\sqrt{s} = 8$ TeV with the ATLAS detector*, *Phys. Rev.* **D 90** (2014) 052008 [arXiv:1407.0608] [INSPIRE].

JHEP05(2016)123

[46] ATLAS collaboration, *ATLAS Run 1 searches for direct pair production of third-generation squarks at the Large Hadron Collider*, *Eur. Phys. J.* **C 75** (2015) 510 [arXiv:1506.08616] [INSPIRE].

[47] ATLAS collaboration, *Search for direct third-generation squark pair production in final states with missing transverse momentum and two b-jets in $\sqrt{s} = 8$ TeV pp collisions with the ATLAS detector*, *JHEP* **10** (2013) 189 [arXiv:1308.2631] [INSPIRE].

[48] CMS collaboration, *Search for top-squark pair production in the single-lepton final state in pp collisions at $\sqrt{s} = 8$ TeV*, *Eur. Phys. J.* **C 73** (2013) 2677 [arXiv:1308.1586] [INSPIRE].

[49] CMS collaboration, *Search for supersymmetry in pp collisions at $\sqrt{s} = 8$ TeV in events with a single lepton, large jet multiplicity and multiple b jets*, *Phys. Lett.* **B 733** (2014) 328 [arXiv:1311.4937] [INSPIRE].

[50] CMS collaboration, *Searches for third-generation squark production in fully hadronic final states in proton-proton collisions at $\sqrt{s} = 8$ TeV*, *JHEP* **06** (2015) 116 [arXiv:1503.08037] [INSPIRE].

[51] CMS collaboration, *Search for supersymmetry in events with soft leptons, low jet multiplicity and missing transverse momentum in proton-proton collisions at $\sqrt{s} = 8$ TeV*, arXiv:1512.08002 [INSPIRE].

[52] OPAL collaboration, G. Abbiendi et al., *Search for stable and longlived massive charged particles in $e^+e^-$ collisions at $\sqrt{s} = 130$ GeV to 209 GeV*, *Phys. Lett.* **B 572** (2003) 8 [hep-ex/0305031] [INSPIRE].

[53] J.A. Casas, J.M. Moreno, K. Rolbiecki and B. Zaldivar, *Implications of light charginos for Higgs observables, LHC searches and dark matter*, *JHEP* **09** (2013) 099 [arXiv:1305.3274] [INSPIRE].

[54] B. Batell, S. Jung and C.E.M. Wagner, *Very light charginos and Higgs decays*, *JHEP* **12** (2013) 075 [arXiv:1309.2297] [INSPIRE].

[55] K. Schmidt-Hoberg and F. Staub, *Enhanced $h \to \gamma\gamma$ rate in MSSM singlet extensions*, *JHEP* **10** (2012) 195 [arXiv:1208.1683] [INSPIRE].

[56] K. Choi, S.H. Im, K.S. Jeong and M. Yamaguchi, *Higgs mixing and diphoton rate enhancement in NMSSM models*, *JHEP* **02** (2013) 090 [arXiv:1211.0875] [INSPIRE].

[57] ATLAS collaboration, *Search for photonic signatures of gauge-mediated supersymmetry in 8 TeV pp collisions with the ATLAS detector*, *Phys. Rev.* **D 92** (2015) 072001 [arXiv:1507.05493] [INSPIRE].

[58] ATLAS collaboration, *Search for direct production of charginos, neutralinos and sleptons in final states with two leptons and missing transverse momentum in pp collisions at $\sqrt{s} = 8$ TeV with the ATLAS detector*, *JHEP* **05** (2014) 071 [arXiv:1403.5294] [INSPIRE].

[59] CMS collaboration, *Searches for electroweak production of charginos, neutralinos and sleptons decaying to leptons and W, Z and Higgs bosons in pp collisions at 8 TeV*, *Eur. Phys. J.* **C 74** (2014) 3036 [arXiv:1405.7570] [INSPIRE].

[60] HEAVY FLAVOR AVERAGING GROUP collaboration, Y. Amhis et al., *Averages of b-hadron, c-hadron and $\tau$-lepton properties as of summer 2014*, arXiv:1412.7515 [INSPIRE].

[61] F. Gabbiani, E. Gabrielli, A. Masiero and L. Silvestrini, *A complete analysis of FCNC and CP constraints in general SUSY extensions of the standard model*, *Nucl. Phys.* **B 477** (1996) 321 [hep-ph/9604387] [INSPIRE].

JHEP05(2016)123